Remarks/Arguments

Claims 35-44, 46-48, and 50-51 are pending in the Application.[1]

Claim 48 is cancelled herein.

Claim 46 is amended herein.

I. EXAMINER INTERVIEW

Applicant greatly appreciates the opportunity to discuss the Final Office Action and background on the technology with the Examiner in a telephone interview on June 7, 2006.

II. NONSTATUTORY DOUBLE PATENTING REJECTIONS

A. United States Patent No. 6,645,455

The Examiner has rejected Claims 35-51 under the judicially created doctrine of obviousness-type double patenting as being unpatentable over Claims 35-36 of United States Patent No. 6,645,455, issued November 11, 2003 to Margrave *et al.* ("the '455 Patent"). Final Office Action, at 2.

Applicant respectfully traverses this rejection. However, to facilitate prosecution of the Application, Applicant hereby responds with the enclosed Terminal Disclaimer to moot this obviousness-type double patenting rejection. Applicant notes that, by filing this terminal disclaimer, it is not admitting the obviousness of the later filed claimed invention claimed in the '455 Patent in light of the earlier filed disclosure of the present Application. *Quad Environmental Tech. v. Union Sanitary Dist.*, 946 F.2d 870, 874, 20 U.S.P.Q.2d 1392, 1394 (Fed. Cir. 1991). Rather, "the filing of a terminal disclaimer simply serves the statutory function of removing the rejection of double patenting, and raises neither presumption nor estoppel on the merits of the rejection." *Id.*, 946 F.2d at 874, 20 U.S.P.Q.2d at 1394-95. And, it is with that understanding Applicant has filed the terminal disclaimer. Therefore, this obviousness-type double patenting rejection is now moot.

[1] In the Final Office Action, Examiner identified Claims 45 and 49 as pending in the Application. Claims 45 and 49 were previously cancelled in Applicant's Amendment Under 37 C.F.R. §1.111, mailed November 14, 2005.

B. United States Patent No. 6,899,945

The Examiner has rejected Claims 35-51 under the judicially created doctrine of obviousness-type double patenting as being unpatentable over Claims 12-24 of United States Patent No. 6,899,945, issued May 31, 2005 to Smalley *et al.* ("the '495 Patent"). Final Office Action, at 2.

Applicant respectfully traverses this rejection. However, to facilitate prosecution of the Application, Applicant hereby responds with the enclosed Terminal Disclaimer to moot this obviousness-type double patenting rejection. Applicant notes that, by filing this terminal disclaimer, it is not admitting the obviousness of the later filed claimed invention claimed in the '495 Patent in light of the earlier filed disclosure of the present Application. *Quad Environmental*, 946 F.2d at 874, 20 U.S.P.Q.2d at 1394. Rather, "the filing of a terminal disclaimer simply serves the statutory function of removing the rejection of double patenting, and raises neither presumption nor estoppel on the merits of the rejection." *Id.*, 946 F.2d at 874, 20 U.S.P.Q.2d at 1394-95. And, it is with that understanding Applicant has filed the terminal disclaimer. Therefore, this obviousness-type double patenting rejection is now moot.

C. United States Patent Application Serial No. 10/730,630

The Examiner has provisionally rejected Claims 35-51 under the judicially created doctrine of obviousness-type double patenting as being unpatentable over Claim 68 of copending United States Patent Application Serial No. 10/730,630 ("the '630 Application"). Office Action, at 2-3.

Applicant respectfully traverses this rejection. However, to facilitate prosecution of the Application, Applicant hereby responds with the enclosed Terminal Disclaimer to moot this obviousness-type double patenting provisional rejection. Applicant notes that, by filing this terminal disclaimer, it is not admitting the obviousness of the later filed claimed invention claimed in the '630 Application in light of the earlier filed disclosure of the present Application. *Quad Environmental*, 946 F.2d at 874, 20 U.S.P.Q.2d at 1394. Rather, "the filing of a terminal disclaimer simply serves the statutory function of removing the rejection of double patenting, and raises neither presumption nor estoppel on the merits of the rejection." *Id.*, 946 F.2d at 874,

20 U.S.P.Q.2d at 1394-95. And, it is with that understanding Applicant has filed the terminal disclaimer. Therefore, this provisional obviousness-type double patenting rejection is now moot.

III. REJECTIONS UNDER 35 U.S.C. § 102(b)/103(a)

Examiner has rejected Claims 35-51 under 35 U.S.C. § 102(b) as being anticipated by or, in the alternative, under 35 U.S.C. § 103(a) as obvious over Ajayan, *et al.*, "Growth morphologies during cobalt-catalyzed single-shell carbon nanotube synthesis" *Chemical Physics Letters,* Vol. 215, No. 5, Dec. 10, 1993, pp. 509-517 ("*Ajayan*"). Final Office Action, at 3.

Examiner contends that *Ajayan* "discloses a material which comprises all single wall carbon nanotubes wherein the nanotubes are in the form of web and/or strings which correspond to the claimed felt/mat and rope." *Id.*

Examiner has rejected Claims 35-51 for anticipation and obviousness. Anticipation under 35 U.S.C. § 102(a) requires each and every element of the claim to be found within the cited prior art reference. To establish a *prima facie* case of obviousness under 35 U.S.C. § 103(a), three basic criteria must be met. First, there must be some suggestion or motivation, either in the references themselves or in the knowledge generally available to one of ordinary skill in the art, to modify the reference or to combine reference teachings. Second, there must be a reasonable expectation of success. Finally, the prior art reference (or references when combined) must teach or suggest all the claim limitations. The teaching or suggestion to make the claimed combination and the reasonable expectation of success must both be found in the prior art and not based on applicant's disclosure. *See* M.P.E.P. 706.02(j); *see also In re Vaeck,* 947 F.2d 488, 20 U.S.P.Q.2d 1438 (Fed. Cir. 1991).

Applicant respectfully traverses the rejections.

Claim 48 is cancelled herein and Claims 45 and 49 were previously cancelled in Applicant's Amendment Under 37 C.F.R. §1.111, mailed November 14, 2005. Thus, the rejections of these claims are moot. As to the remaining claims:

Regarding Claim 35, this independent claim requires a rope of single-wall carbon nanotubes having 50 to 5000 single-wall carbon nanotubes of which greater than 10% are (10,10) single-wall carbon nanotubes. *Ajayan* does not teach or suggest all the elements of this

claim. *Ajayan* does not teach or suggest a rope of single-wall carbon nanotubes having 50 to 5000 single-wall carbon nanotubes of which greater than 10% are (10,10) single-wall carbon nanotubes, let alone any particular, specific (n,m) tube configuration.

Applicant notes that, in the Application, Applicant has used the nomenclature described by M.S. Dresselhaus, G. Dresselhaus, and P.C. Eklund, *Science of Fullerenes and Carbon Nanotubes*, Chap. 19, (1996), published by Academic Press, 525 B Street, Suite 1900, San Diego, California 92101-4495 or 6277 Sea Harbor Drive, Orlando, Florida 32877 (ISBN 0-12-221820-5), ("*Dresselhaus*"), which was incorporated in the Application by reference. (Application at 6, *ll.* 8-14) Thus, a (10,10) single-wall carbon nanotube is a specific type of single-wall carbon nanotube.

Examiner has stated that because of similarities in the diameters of the single-wall carbon nanotubes, the composition of *Ajayan* would possess greater than 10% of (10,10) single-wall carbon nanotubes. (*See* Final Office Action, at 3-4). Applicant does not and cannot concur. Although *Ajayan* discloses a nanotube diameter, the diameter of a nanotube is generally not indicative of a particular tube configuration. For any given tube configuration, there is a unique diameter, however, *the converse is not true.* In fact, there are a number of (n, m) tube configurations that can produce a tube of a particular diameter or in a particular diameter range. (*See* Iijma, et al., "Single-shell carbon nanotubes of 1-nm diameter," *Nature*, 363, June 17, 1993, pp. 603-605, ("*Iijima*"), attached as **Exhibit A**.) In particular, see hatched areas in Figure 2 of *Iijima*. The hatched areas are indicative of nanotubes with diameters of around 0.8 nm and around 1.05 nm. The particular (n,m) configuration determines the diameter of the single-wall carbon nanotube.

There are many (n,m) configurations that can give similar nanotube diameters, as shown by *Iijima* in Figure 2. Furthermore, single-wall carbon nanotubes of various (n,m) configurations can have very similar diameters. This statement can easily be shown by calculating the diameters of various carbon nanotubes with different (n,m) tube configurations according to the following equation. (*See Dresselhaus*, page 760)

$$d_t = \sqrt{3}\ a_{C\text{-}C}\,(m^2 + mn + n^2)^{1/2}/\pi$$

where d_t is the nanotube diameter in Angstroms and
$a_{C\text{-}C}$ is the nearest-neighbor C-C distance (1.421 Å in graphite).

The calculation of diameter has been done for various (n,m) nanotube configurations and the results are tabulated in **Exhibit B**. This demonstrates that a nanotube having a particular (n,m) configuration has a unique diameter, however, there are multiple (n,m) tube configurations that can have approximately the same tube diameters. Hence, a particular diameter of nanotube cannot be equated, *a priori*, to a particular (n,m) tube configuration.

To further illustrate this point, Applicant is attaching hereto as **Exhibit C** the following non-prior art article: Kim, *et al.*, "Synthesis of Ultralong and High Percentage of Semiconducting Single-walled Carbon Nanotubes," *Nano Lett.*, **2002**, Vol. 2, No. 7, 703-708 ("*Kim*"). *Kim* shows that, unless a process is specifically tailored to make single-wall carbon nanotubes having preferred (n,m) indices, then of all the single-wall carbon nanotubes produced in the range of 1 to 2 nm, less than 4.6% would be expected to be (n,n) single-wall carbon nanotubes (M-SWNT), and less than 0.7% would be expected to be (10, 10) single-wall carbon nanotubes. *See Kim*, at 705, col. 2, and at 706 (including Table 1). In Table 1, *Kim* presents the theoretically possible number of (n,n) tubes (M-SWNT) in various diameter ranges. The possible number of different single-wall carbon nanotube configurations in the range of 1 to 2 nm is 153, and out of that number, only 7 of these 153 (less than 4.6%) are (n,n) single-wall carbon nanotubes and only 1 out of 153 (less than 0.7%) is a (10,10) single-wall carbon nanotube.[2]

Therefore, *Kim* shows that, in the absence of a production-driven preference for a particular (n,m) or group of (n,m) values, of which (10, 10) is the subject of the presently

[2] As reflected in Exhibit B, there are at least 49 different single-wall carbon nanotube configurations having diameters between 1.1 and 1.4 nm. Thus, for this range and without preference, less than 2.1% would be (10,10) single-wall carbon nanotubes. As further reflected in Exhibit B, there are at least 25 different single-wall carbon nanotube configurations having diameters between 1.2 and 1.3 nm. Interestingly, the (10,10) single-wall carbon nanotube configuration does not fall within this range. However if this configuration were within the range, less than 3.9% would be (10,10) single-wall carbon nanotubes.

claimed invention, the concentration of (10,10) single-wall carbon nanotubes is much less than 10% of the total possible nanotube (n,m) configurations. This strongly supports that, in the absence of special processing parameters and steps to produce compositions having a high level of (10, 10) single-wall carbon nanotubes, *Ajayan* would not have produced compositions having an unusually high concentration of (10, 10) single-wall carbon nanotubes. Moreover, *Ajayan's* silence on this issue suggests that no special processing steps were undertaken or achieved.

Thus, *Ajayan* does not teach or suggest a rope of single-wall carbon nanotubes having 50 to 5000 single-wall carbon nanotubes of which greater than 10% are (10,10) single-wall carbon nanotubes. *Ajayan* does not teach or suggest any particular (n,m) configuration of single-wall carbon nanotube, nor does *Ajayan* teach any particular concentration of said configuration. As *Ajayan* does not teach or suggest each and every element of this claim, Claim 35 cannot be anticipated by *Ajayan.* Furthermore, there is no suggestion or motivation in *Ajayan*, or in the knowledge generally available to one of ordinary skill in the art, to modify the reference to include and/or yield such elements. Consequently, a *prima facie* case of obviousness has not been established and, thus, the claim cannot be held obvious under 35 U.S.C. § 103(a).

Regarding Claims 36-44, these claims are dependent directly or indirectly upon independent Claim 35 and are not anticipated by, or obvious over *Ajayan* for the same reasons Claim 35 is not anticipated by, or obvious over *Ajayan.*

Regarding Claim 46, this claim has been amended to incorporate the requirements of Claim 35 and, thus, require a felt comprising single-wall carbon nanotubes wherein the single-wall carbon nanotubes comprise ropes of single-wall nanotubes, wherein greater than 10% of the single-wall carbon nanotubes are (10, 10) single-wall carbon nanotubes, and wherein said felt is electrically conductive. No new matter is added by virtue of this amendment. Support for this amendment is found in the Application at page 23, *ll.* 20-29 to page 24, *ll.* 1-14.

Since Claim 46 has been amended to incorporate the requirements of Claim 35, Claim 46, as amended, is not anticipated by or obvious over *Ajayan* for the same reasons that Claim 35 is not anticipated by or obvious over *Ajayan. Ajayan* does not teach or suggest a felt of single-wall carbon nanotubes, wherein the single-wall carbon nanotubes comprise ropes of single-wall

nanotubes, wherein greater than 10% of the single-wall carbon nanotubes are (10,10) single-wall carbon nanotubes, and wherein the felt is electrically conductive. *Ajayan* does not teach or suggest any specific (n,m) tube configuration, nor does *Ajayan* teach any particular concentration of said configuration, and, therefore, *Ajayan* does not teach or suggest all the elements of amended Claim 46. Furthermore, there is no suggestion or motivation in *Ajayan*, or in the knowledge generally available to one of ordinary skill in the art, to modify the reference to include such elements. Consequently, a *prima facie* case of obviousness has not been established and, thus, the claim cannot be held obvious under 35 U.S.C. § 103(a).

Regarding Claims 47 and 50-51, these claims are dependent directly upon amended independent Claim 46 and are not anticipated by, or obvious over *Ajayan* for the same reasons Claim 46 is not anticipated by, or obvious over *Ajayan.*

Therefore, as a result of the foregoing, Applicant respectfully requests that the Examiner withdraw the rejection of Claims 35-44, 46-47 and 50-51 under 35 U.S.C. § 102(b) as being anticipated by, or in the alternative, under 35 U.S.C. § 103(a) as obvious over *Ajayan.*

III. CONCLUSION

As a result of the foregoing, it is asserted by Applicant that the Claims in the Application are now in a condition for allowance, and respectfully requests allowance of such Claims. Applicant respectfully requests that the Examiner call Applicant's attorney at the below listed number if the Examiner believes that such a discussion would be helpful in resolving any remaining problems.

Respectfully submitted,

WINSTEAD SECHREST & MINICK P.C.
Attorneys for Applicant

By: _____
Ross Spencer Garsson
Reg. No. 38,150

P.O. Box 50784
Dallas, Texas 75201
(512) 370-2870

Single-shell carbon nanotubes of 1-nm diameter

Sumio Iijima & Toshinari Ichihashi

Fundamental Research Laboratories, NEC Corporation, 34 Miyukigaoka, Tsukuba, Ibaraki 305, Japan

CARBON nanotubes[1] are expected to have a wide variety of interesting properties. Capillarity in open tubes has already been demonstrated[2-5], while predictions regarding their electronic structure[6-8] and mechanical strength[9] remain to be tested. To examine the properties of these structures, one needs tubes with well defined morphologies, length, thickness and a number of concentric shells; but the normal carbon-arc synthesis[10,11] yields a range of tube types. In particular, most calculations have been concerned with single-shell tubes, whereas the carbon-arc synthesis produces almost entirely multi-shell tubes. Here we report the synthesis of abundant single-shell tubes with diameters of about one nanometre. Whereas the multi-shell nanotubes are formed on the carbon cathode, these single-shell tubes grow in the gas phase. Electron diffraction from a single tube allows us to confirm the helical arrangement of carbon hexagons deduced previously for multi-shell tubes[1].

We found the single-shell tubules in soot-like deposits formed in a carbon-arc chamber similar to that used for fullerene production. Two vertical electrodes are installed in the centre of the chamber. The anode, which is the upper electrode, is a graphitic carbon rod 10 mm in diameter, and the cathode, a 20-mm-diameter carbon rod, has a shallow dimple used to hold a small piece of iron during evaporation. The evaporation chamber is filled with a gas mixture typically consisting of 10 torr methane and 40 torr argon. The carbon discharge arc was generated by running a d.c. current of 200 A at 20 V between the electrodes. The iron filings melted to form a droplet, and so generated iron vapour which cooled and condensed into small particles of iron carbide above the cathode. The vaporization of iron takes place simultaneously with the production of soot, both from methane and by evaporation from the carbon cathode. We noticed that no tubules were formed when the carbon arc reactor was operated with any one of the three components argon, iron and methane absent.

The catalytic role of iron is well known in carbon fibre production, in which iron particles are found on the fibre tips and act as heterogeneous deposition centres for carbon atoms from the vapour phase[12]. In the present experiment, we did not find iron particles at the tubule tips. We suspect, however, that atomic iron particles, presumably as a homogeneous catalyst in the vapour phase, somehow assist the formation of single-shell tubules. Specimens for electron microscopy were prepared from acetone suspensions of soot collected over the electrodes in the evaporation chamber. Nanotubes were placed on a microscope specimen grid by drying a drop of the suspension taken up on the grid. We used either an ultra-high-vacuum (JEM 200FXV) or conventional transmission electron microscope (Topcon 002B) at 120 kV or 200 kV accelerating voltage.

A typical electron micrograph showing a general view of the specimen is reproduced in Fig. 1*a*. Threads are curved and tangled together to form bundles in some regions. All the threads are found to be single-shell carbon nanotubes. Round, dark objects attached to the tubules are cementite (Fe_3C), as indicated by powder diffraction measurements and measurement of the *d* spacings of lattice fringes (lattice images with spacings of around 0.2 nm were recorded on individual particles); these particles range in size from a few nanometres to several tens of nanometres, which were mostly coated with a few graphite layers. Some of the particles were soluble in nitric acid.

The nanotubes often form as bundles, but isolated and single tubules are also present. Three tubules which bridge two cementite particle agglomerates are seen in Fig. 1*b*. On the upper right-hand side, a graphitic layer showing an image of the basal plane with lattice spacing 0.34 nm can be recognized. From this, we calibrated the magnifications of the tubules. All micrographs were recorded at optimum focus[13], so that two dark lines in the tubule image correspond to side portions of the cylinders. The thinnest tube in this micrograph (labelled 1) is 0.75 nm in diameter, and is attached to a thicker (13-nm) tube (labelled 2). Tubules 1 and 2 are slightly curved, but tubule 3 (diameter 0.92 nm) spans straight across a 140-nm opening between two cementite particle agglomerates. The longest single-shell tubule was 700 nm long with a diameter of 0.9 nm.

Short and terminated tubules are commonly observed (4 and 5 in Fig. 1*b*). The terminated tubule labelled 6 moved gradually during the observation so that one end appears to be fading out. No cementite particles were found on the free tips of the tubules, but they are entangled with cementite particle agglomerates. The tubules are capped in shapes that have been reported previously[14,15] (arrow 4 in Fig. 2).

We carefully measured the diameters on the electron micrographs of individual tubules. Figure 2 shows a histogram of the diameters of about 60 tubules, which range from about 0.7 nm to 1.6 nm. Two peaks are seen at tubule diameters of around 0.8 nm and 1.05 nm; we believe that these peaks are significant. The origin of the preferred tubule diameters is interesting to consider in terms of the tubule helicity and growth.

Figure 3*a* shows an electron diffraction pattern taken from a 1.37-nm single-shell tubule together with its corresponding

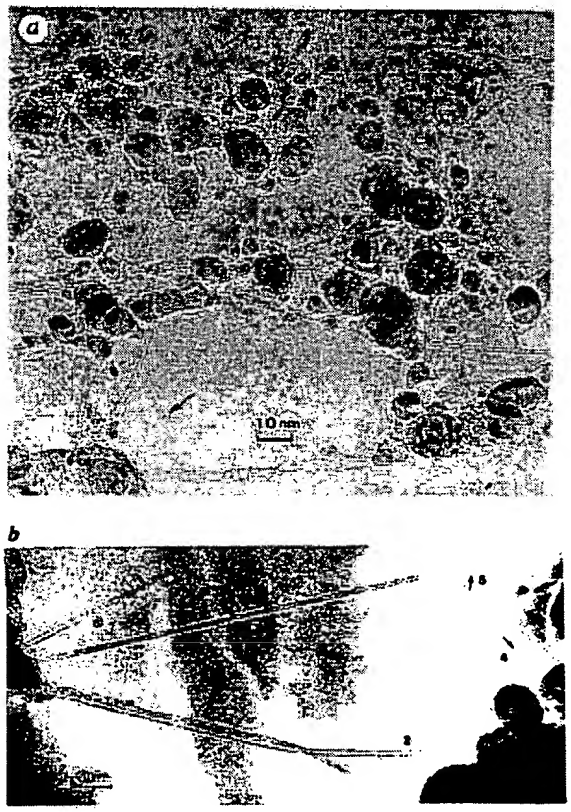

FIG. 1*a*, Electron micrograph showing bundles of single-shell carbon nanotubes which are curved and entangled. Dark blobs are cementite particles which assist in tubule growth. A terminated tubule is indicated by an arrow. *b*, Electron micrograph showing individual single-shell nanotubes. The tubule labelled 1 is 0.75 nm in diameter and tubule 2 is 1.37 nm in diameter. A straight tubule (3) and two terminated ones (4 and 5) can also be seen.

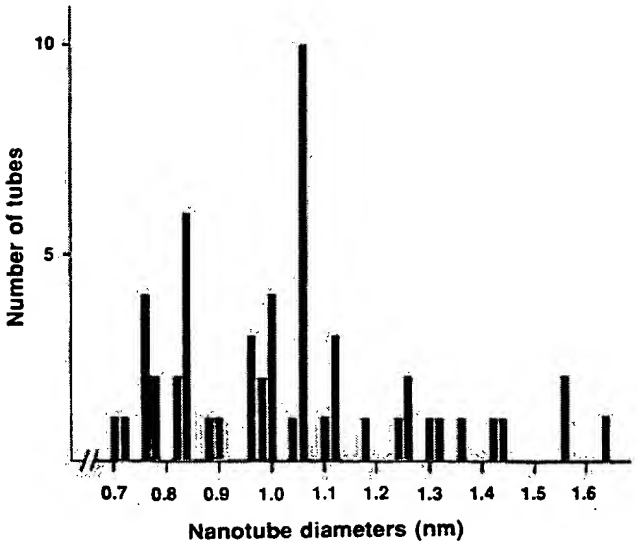

FIG. 2 Histogram showing frequency of single-shell nanotubes of different tubule diameters. Two peaks, at 0.8 nm and 1.35 nm, are dominant.

electron micrograph (Fig. 3*b*). The tubule is attached to the bundle of tubules seen at the left-hand side. An electron beam (20 nm diameter) was focused on to the tubule, so that the area diffracting the electrons comprised about 2,000 carbon atoms. This small scattering volume and the cylindrical structure are responsible for the extremely weak and diffused diffraction intensities. There are two hexagonal (*hk*0) diffraction patterns rotated ± $\alpha/2$ from perfect alignment along the tube axis, and these patterns show mirror symmetry both along and perpendicular to the tube axis. The mirror symmetry confirms helicity in the single-shell tubule structure, as was found previously for multi-shell tubules[1]. All electron diffraction patterns observed in the present sample showed the 2*mm* symmetry. The (00*l*) spots coming from the graphite basal lattice plane, which were observed for the multi-shell tubes, are completely absent (see Fig. 3 of ref. 1).

The spots are streaked vertically because of the fibrous structure. Each streaked spot in Fig. 3*a* has intensity maxima appearing with a period (indicated by triple arrows) of 0.73 nm^{-1}. The value corresponds to the diameter measured on the tubule (1.37 nm). The modulation can be explained by Fraunhofer diffraction from two vertical portions of the tubule

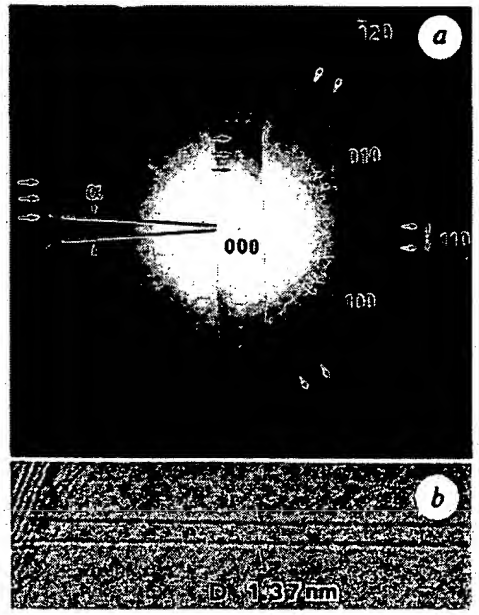

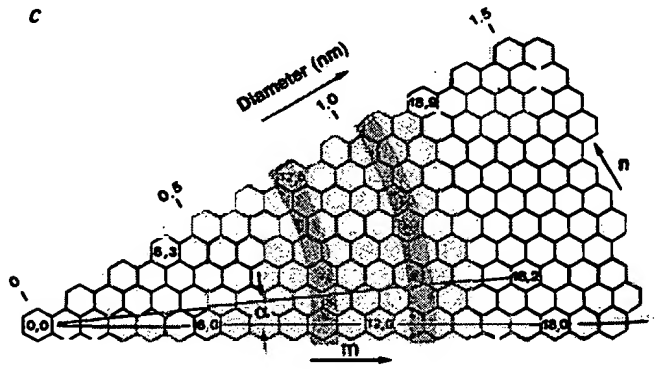

FIG. 3*a*, Electron diffraction pattern taken from a single-shell nanotubule of diameter 1.37 nm. *b*, Electron micrograph of same tubule. The pattern comprises two sets of the hexagonal patterns which gives rise to splitting of the (*hk*0) spots. Each spot has periodic intensity maxima in the vertical direction, caused by Fraunhofer diffraction from the two portions of the tube imaged as two dark lines in *b*. *c*, Schematic representation of helical tubules according to Hamada's notation[6]. A tubule is represented by an index (*m*, *n*) or (*m*, α), where *m* is *m*th hexagon from the origin (0, 0), and *n* and α are defined as shown. α is a pitch angle. If the tubule diameter *D* and angle α are known, the tubule structure is uniquely determined. Hatched hexagons represent the tubules corresponding to the two peaks in Fig. 2.

parallel to the incident electron waves.

By knowing the tubule diameter D and its pitch angle α with respect to the fibre axis (Fig. 3*a*), the helicity and thus the tubule structure can be determined uniquely. To describe the tubule helicity, we follow Hamada's notation[6] as illustrated in Fig. 3*c*, where a tubule can be represented by an index (m, n). This tubule can be realized by rolling up a sheet of hexagons so as to superimpose the origin (0, 0) on the hexagon (m, n). A tubule $(m, -n)$ is chiral with the opposite handedness to (m, n), and thus they should be optically active, but they cannot be distinguished by the diffraction experiment. The tubules which were observed frequently on the histogram (Fig. 2) have values of (m, n) in the hatched areas. On the electron diffraction pattern in Fig. 3*a*, α and D are measured as 7° and 1.37 nm, respectively. This tube can be indexed as (18, 2) or its enantiomer (18, −2), and should behave as a semiconductor according to electronic band structure calculations[6,16]. We should mention here that α, or helicity, varies for a given tubule diameter.

We speculate that the single-shell tubules might be the embryo for the multi-shell tubules. In our proposed model for the nanotube growth[17,18], the tubule ends are open so that carbon atoms are easily captured at dangling bonds, and the multi-shell tubules grow in the direction of the tube axis and also perpendicular to it. The latter growth is associated with layer-by-layer growth on the tubule surface. In the single-shell tubes, we assume that axial growth dominates over layer growth. We speculate that the iron in the present experiments acts as a homogeneous catalyst in the vapour phase. □

Received 23 April; accepted 1 June 1993.

1. Iijima, S. *Nature* **354**, 56–58 (1991).
2. Ajayan, P. M. & Iijima, S. *Nature* **361**, 333–334 (1993).
3. Ajayan, P. M. *et al. Nature* **362**, 522–523 (1993).
4. Tsang, S.C., Harris, P.J. F. & Green, M.L. *Nature* **362**, 520–522 (1993).
5. Pederson, M. R. & Broughton, J. O. *Phys. Rev. Lett.*, **69**, 2687–2692 (1992).
6. Hamada, N., Sawada, S. & Oshiyama, S. *Phys. Rev. Lett.* **68**, 1579–1581 (1992).
7. Mintmire, J. W., Dunlap, B. I. & White, C. T. *Phys. Rev. Lett.* **68**, 631–634 (1992).
8. Saito, R., Fujita, F., Dresselhaus, G. & Dresselhaus, M. S. *Phys. Rev.* B **46**, 1804–1811 (1992).
9. Robertson, D. H., Brenner, D. W. & Mintmire, J. W. *Phys. Rev.* B **45**, 12592–12595 (1992).
10. Ebbesen, T.W. & Ajayan, P.M. *Nature* **358**, 220–222 (1992).
11. Ando, Y. & Iijima, S. *Jpn. J. appl. Phys.* **32**, L107–L109 (1993).
12. Oberlin, A. & Endo, M. *J. Cryst. Growth* **32**, 335–349 (1976).
13. Iijima, S. *Chem. Scripta* **14**, 117–123 (1978-79).
14. Iijima, S., Ichihashi, T. & Ando, Y. *Nature* **356**, 776–778 (1992).
15. Ajayan, P.M. Ichihashi, T. & Iijima, S. *Chem. Phys. Lett.* **202**, 384–388 (1992).
16. White, C. T., Robertson, D. H. & Mintmire, J. W. *Phys. Rev.* B **47**, 5485–5488 (1993).
17. Iijima, S., Ajayan, P. M. & Ichihashi, T. *Phys. Rev. Lett.* **69**, 3100–3103 (1992).
18. Iijima, S. *Mat. Sci. Enging* B. (in the press).

EXHIBIT B

Diameters of Single-Wall Carbon Nanotubes as a function of (n,m) Configuration

(n, m)	n	m	a of C-C	3' 1/2	pi		Diameter (Angstrom)	Diameter (nm)
			1.421	1.73205	3.14159			
5,5	5	5	1.421	1.73205	3.14159		6.78	0.678
9,0	9	0	1.421	1.73205	3.14159		7.05	0.705
6,5	6	5	1.421	1.73205	3.14159		7.47	0.747
7,4	7	4	1.421	1.73205	3.14159		7.56	0.756
8,3	8	3	1.421	1.73205	3.14159		7.72	0.772
10,0	10	0	1.421	1.73205	3.14159		7.83	0.783
9,2	9	2	1.421	1.73205	3.14159		7.95	0.795
6,6	6	6	1.421	1.73205	3.14159		8.14	0.814
7,5	7	5	1.421	1.73205	3.14159		8.18	0.818
10,1	10	1	1.421	1.73205	3.14159		8.25	0.825
8,4	8	4	1.421	1.73205	3.14159		8.29	0.829
9,3	9	3	1.421	1.73205	3.14159		8.47	0.847
11,0	11	0	1.421	1.73205	3.14159		8.62	0.862
10,2	10	2	1.421	1.73205	3.14159		8.72	0.872
6,7	6	7	1.421	1.73205	3.14159		8.83	0.883
8,5	8	5	1.421	1.73205	3.14159		8.90	0.890
11,1	11	1	1.421	1.73205	3.14159		9.04	0.904
9,4	9	4	1.421	1.73205	3.14159		9.04	0.904
10,3	10	3	1.421	1.73205	3.14159		9.24	0.924
12,0	12	0	1.421	1.73205	3.14159		9.40	0.940
11,2	11	2	1.421	1.73205	3.14159		9.50	0.950
7,7	7	7	1.421	1.73205	3.14159		9.50	0.950
6,8	6	8	1.421	1.73205	3.14159		9.53	0.953
9,5	9	5	1.421	1.73205	3.14159		9.63	0.963
10,4	10	4	1.421	1.73205	3.14159		9.79	0.979
12,1	12	1	1.421	1.73205	3.14159		9.82	0.982
11,3	11	3	1.421	1.73205	3.14159		10.00	1.000
8,7	8	7	1.421	1.73205	3.14159		10.18	1.018
13,0	13	0	1.421	1.73205	3.14159		10.18	1.018
12,2	12	2	1.421	1.73205	3.14159		10.27	1.027
10,5	10	5	1.421	1.73205	3.14159		10.36	1.036
11,4	11	4	1.421	1.73205	3.14159		10.54	1.054
13,1	13	1	1.421	1.73205	3.14159		10.60	1.060
12,3	12	3	1.421	1.73205	3.14159		10.77	1.077
8,8	8	8	1.421	1.73205	3.14159		10.86	1.086
9,7	9	7	1.421	1.73205	3.14159		10.88	1.088
10,6	10	6	1.421	1.73205	3.14159		10.97	1.097
14,0	14	0	1.421	1.73205	3.14159		10.97	1.097
13,2	13	2	1.421	1.73205	3.14159		11.05	1.105
11,5	11	5	1.421	1.73205	3.14159		11.11	1.111
12,4	12	4	1.421	1.73205	3.14159		11.30	1.130
14,1	14	1	1.421	1.73205	3.14159		11.38	1.138
13,3	13	3	1.421	1.73205	3.14159		11.54	1.154
10,7	10	7	1.421	1.73205	3.14159		11.59	1.159
11,6	11	6	1.421	1.73205	3.14159		11.70	1.170
15,0	15	0	1.421	1.73205	3.14159		11.75	1.175

EXHIBIT B

Diameters of Single-Wall Carbon Nanotubes as a function of (n,m) Configuration

14,2	14	2	1.421	1.73205	3.14159		11.83	1.183
12,5	12	5	1.421	1.73205	3.14159		11.86	1.186
13,4	13	4	1.421	1.73205	3.14159		12.06	1.206
15,1	15	1	1.421	1.73205	3.14159		12.16	1.216
10,8	10	8	1.421	1.73205	3.14159		12.24	1.224
11,7	11	7	1.421	1.73205	3.14159		12.31	1.231
14,3	14	3	1.421	1.73205	3.14159		12.31	1.231
12,6	12	6	1.421	1.73205	3.14159		12.44	1.244
16,0	16	0	1.421	1.73205	3.14159		12.54	1.254
13,5	13	5	1.421	1.73205	3.14159		12.61	1.261
15,2	15	2	1.421	1.73205	3.14159		12.61	1.261
14,4	14	4	1.421	1.73205	3.14159		12.83	1.283
10,9	10	9	1.421	1.73205	3.14159		12.90	1.290
11,8	11	8	1.421	1.73205	3.14159		12.94	1.294
16,1	16	1	1.421	1.73205	3.14159		12.94	1.294
12,7	12	7	1.421	1.73205	3.14159		13.04	1.304
15,3	15	3	1.421	1.73205	3.14159		13.09	1.309
13,6	13	6	1.421	1.73205	3.14159		13.18	1.318
17,0	17	0	1.421	1.73205	3.14159		13.32	1.332
14,5	14	5	1.421	1.73205	3.14159		13.36	1.336
16,2	16	2	1.421	1.73205	3.14159		13.39	1.339
10,10	10	10	1.421	1.73205	3.14159		13.57	1.357
11,9	11	9	1.421	1.73205	3.14159		13.59	1.359
15,4	15	4	1.421	1.73205	3.14159		13.59	1.359
17,1	17	1	1.421	1.73205	3.14159		13.73	1.373
13,7	13	7	1.421	1.73205	3.14159		13.77	1.377
16,3	16	3	1.421	1.73205	3.14159		13.86	1.386
14,6	14	6	1.421	1.73205	3.14159		13.93	1.393
18,0	18	0	1.421	1.73205	3.14159		14.10	1.410
15,5	15	5	1.421	1.73205	3.14159		14.12	1.412
17,2	17	2	1.421	1.73205	3.14159		14.17	1.417
11,10	11	10	1.421	1.73205	3.14159		14.25	1.425
12,9	12	9	1.421	1.73205	3.14159		14.30	1.430
13,8	13	8	1.421	1.73205	3.14159		14.38	1.438
14,7	14	7	1.421	1.73205	3.14159		14.51	1.451
11,11	11	11	1.421	1.73205	3.14159		14.93	1.493
12,10	12	10	1.421	1.73205	3.14159		14.95	1.495
13,9	13	9	1.421	1.73205	3.14159		15.01	1.501

NANO LETTERS

2002
Vol. 2, No. 7
703−708

Synthesis of Ultralong and High Percentage of Semiconducting Single-walled Carbon Nanotubes

Woong Kim, Hee Cheul Choi, Moonsub Shim, Yiming Li, Dunwei Wang, and Hongjie Dai*

Department of Chemistry, Stanford University, Stanford, California 94305

Received May 2, 2002; Revised Manuscript Received May 15, 2002

ABSTRACT

Two main results are reported here for single-walled carbon nanotubes (SWNTs) synthesized from well-controlled isolated catalytic Fe_2O_3 nanoparticles. The first is patterned growth of ultralong SWNTs (lengths up to 0.6 millimeters) by using a mixed methane and ethylene carbon source in chemical vapor deposition (CVD). Interesting loop and closed ring structures similar to those of fullerene "crop circles" are observed on these as-grown ultralong tubes. Second, surveying the electronic properties of individual SWNTs by transport measurements reveals that approximately 70% of individual SWNTs grown from isolated nanoparticles are semiconductors exhibiting field effect transistor (FET) characteristics. The distribution of CVD-grown SWNT chirality is elucidated for the first time, and implications to array-based nanotube electronics and sensors are discussed.

The synthesis of single-walled carbon nanotubes has recently been carried out with isolated discrete catalytic nanoparticles carefully derived by wet chemical routes, aimed at controlling the structure (e.g., diameter) of these novel nanowires.[1−3] The highly sensitive structure−property relations[4] in nanotubes require control of nanotube diameter and chirality in order to predict the growth of metallic or semiconducting molecular wires. Although not yet at hand, a path to such control could be via the control of catalytic "seeds" and understanding how seed particles determine the nanotube diameter and chirality.[5,6] Progress has indeed been made along this line. With powder-based supported catalyst, SWNTs synthesized by CVD have a wide diameter distribution of 1−5 nm. Using isolated nanoparticles synthesized in apoferritin as catalyst, one can narrow down the diameters of CVD-grown nanotubes to 1−3 nm.[1] Further narrowing of the diameters of CVD tubes to 1−2 nm is achieved recently using nanoparticles derived on dendrimer templates.[7]

This letter follows up on the synthesis and properties of SWNTs grown from ferritin. New structural data of nanotubes is obtained, and the electronic properties of isolated SWNTs are surveyed statistically. The results include the growth of SWNTs into macroscopic lengths up to 0.6 mm, the longest reported for isolated single-walled tubes. The nanotubes exhibit interesting loop and ring morphologies in their as-grown forms. Multiprobe transport study reveals no apparent changes in chirality along the lengths of these long tubes. Measurements over large numbers of individual SWNTs reveal that about 70% of the nanotubes are semiconductors and others being small band gap semiconductors and metals. The results combined with structure−property analysis suggest that SWNTs grown from our current method in fact do not favor any tube chirality. Nevertheless, the high yield and "natural abundance" of semiconducting nanotubes in the synthesis is welcome and can be exploited in building large arrays of nanotube transistors and sensors.

The synthesis of Fe_2O_3 nanoparticles with ferritin has been described previously.[1] We deposit ferritin from a 1.6 μM water solution into an array of square wells[8,9] of polymethylmathacrylate (PMMA) patterned photolithographically on a SiO_2 substrate by incubating the substrate in the ferritin solution for 2 h. Liftoff of PMMA followed by calcination[1] in air results in a submonolayer of catalytic Fe_2O_3 nanoparticles confined in square regions (side length 0.1−3 μm) on SiO_2. Nanotube growth on the substrate takes place in a 1 in. tube-furnace at 900 °C for 10 min under combined flows of 1000 sccm (standard cubic centimeter per minute) of CH_4 (99.999%, gas correction factor 0.72), 500 sccm of H_2 (gas correction factor 1.01), and 20 sccm of C_2H_4 (gas correction factor 0.60). Note that the combination of gases here differs slightly from our previous recipe for SWNT growth.[1,8,9]

Atomic force microscopy (AFM) imaging reveals that SWNTs are reliably grown and emanating from the patterned catalyst sites. The average number of nanotubes grown from each square decorated by Fe_2O_3 nanoparticles is 1−5. Statistics show about 30% of the isolated nanotubes grown on a substrate are very long, with lengths ≥ 100 μm, and

* Corresponding author. Phone: (650) 723-4518. Fax: (650) 725-0259. E-mail: hdai1@stanford.edu.

10.1021/nl025602q CCC: $22.00
Published on Web 06/01/2002

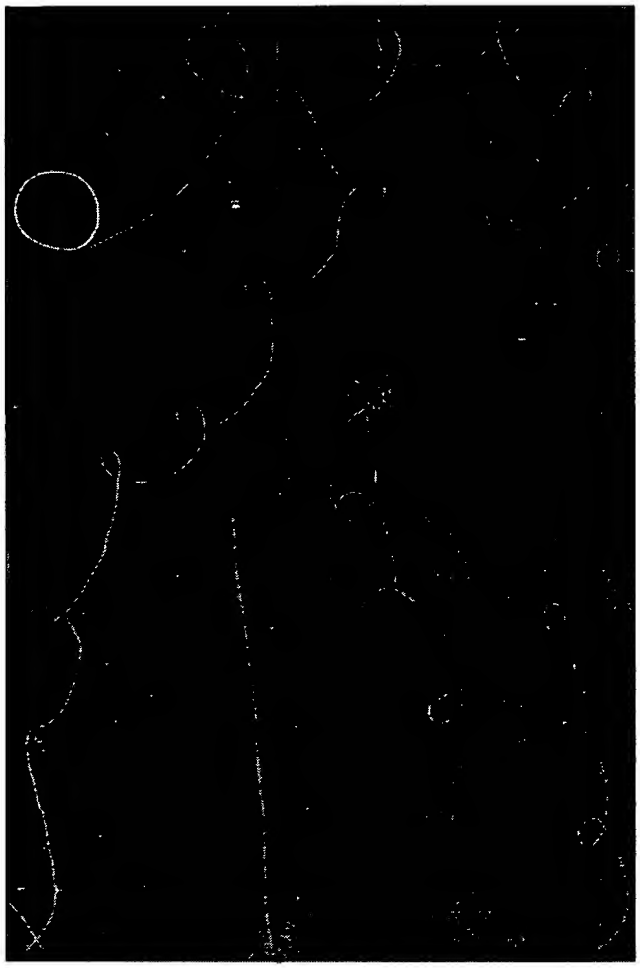

Figure 1. Very long as-grown single-walled carbon nanotubes. (a) A mosaic of AFM images for a 320 μm long nanotube (diameter ~2 nm). The nanotube is grown from a catalyst particle in a patterned region circled at the bottom of the figure. See text for the formation of loop structures. (b) AFM image of a 40 μm long straight nanotube grown from a patterned catalyst site (circled at the bottom). (c) AFM image of a 110 μm long nanotube. (d) AFM image showing a closed ring near the extended end of a long tube.

the longest SWNT observed is ~600 μm. Figure 1a is a mosaic of AFM images showing a 320 μm long SWNT (diameter = 2 nm) grown from a catalyst square (circled region at the bottom of Figure 1a). The nanotube exhibits 14 oval-shaped loops (diameters ~ 2 μm) along its length (the last tube section is not shown, limited by figure size). While nanotubes tens of microns long are typically relatively straight (Figure 1b), tubes that are hundreds of microns long tend to show loop structures along their length. A second example is shown in Figure 1c in which a 110 μm long nanotube contains 7 loops.

Completely closed ring structures are observed on about 5−10% of the very long nanotubes. Shown in Figure 1d is the end section of a 160 μm long nanotube containing such a ring with a topographic height along its circumference ~10 nm (high brightness) compared to the 2.2 nm height along the rest of the tube. It can be gleaned that the ring is formed by the nanotube looping around for about 10 turns into a circular self-bundle. At the end of the nanotube, there is a 380 nm long segment not included into the bundle structure, as it branches off from the ring (Figure 1d). The loop and closed ring structures here are observed with as-grown SWNTs, different from those observed after post-growth treatment in liquids.[10−12]

The loops and rings are most likely formed in free space during SWNTs growth before they land on the substrate. As a SWNT grows out from the substrate into space, with a high aspect ratio of $>10^5$, it can loop around to cross itself to form van der Waals (vdW) point contacts, or loop around multiple times to make vdW line contacts with itself to form a ring. The vdW contacting and thermal energies overcome mechanical bending energy of the nanotube, leading to stable formation of loop and ring structures. The persistence length of a SWNT is ~0.8 μm,[12] and thermal energy at the high growth temperature is sufficient to cause nanotube looping with a radius on the order of ~1 μm. There is a possibility that the loop structures are formed when a loop-free and relatively straight tube in free space contacts a substrate. This explanation, however, is not plausible for the formation of closed rings with multiple loops.

The growth condition for isolated long SWNTs is robust and reproducible. Methane, hydrogen, and ethylene flows are balanced to enable continuous carbon feeding and nanotube growth while preventing catalyst poisoning by amorphous carbon deposition. We have not been able to grow similar yield of long tubes with methane or ethylene alone, suggesting that the combination of methane and ethylene is important to provide efficient carbon feedstock needed for nanotube growth. On the other hand, balancing with hydrogen[13] prevents excess carbon deposition from poisoning the catalyst and sustains nanotube growth over an extended period of time. Long SWNTs have been synthesized previously by using methane and a conditioning approach that generates higher hydrocarbons in situ,[14] which motivates the current growth condition with the intentional addition of ethylene. The results here provide important information about the growth rate of SWNTs in CVD. A SWNT can grow at >60 μm/min, and a reaction time of 10 s can already produce nanotubes with micron scale length in CVD. Typical transmission electron microscopy (TEM) data are shown in Figure 2 to confirm[1,2] that the nanotubes are indeed single-walled.

Next, we focus on elucidating the physical properties of SWNTs thus produced. Device fabrication involves microfabrication with the substrates containing SWNTs emanating from well-defined surface sites.[9] Titanium is used as electrodes for contacting nanotubes, and the Si substrate under the SiO_2 surface layer is used as a gate. We have carried out multiprobe (Figure 3a,b) electrical measurements on a total of 9 SWNTs with lengths >100 μm. Eight out of the nine tubes are found to be semiconductors exhibiting FET characteristics. Figure 3c,d shows the current vs gate ($I-V_g$) curves for a 700 nm long straight and a 21 μm long loop segments respectively on a long tube. Both segments exhibit hole-carrier depletion by positive gate, typical of p-type semiconductors.[15,16] The transconductance dI/dV_g for the short and straight segments is 1.7×10^{-7} A/V with a resistance of 95 kΩ at $V_g = -10$ V. Transconductance for

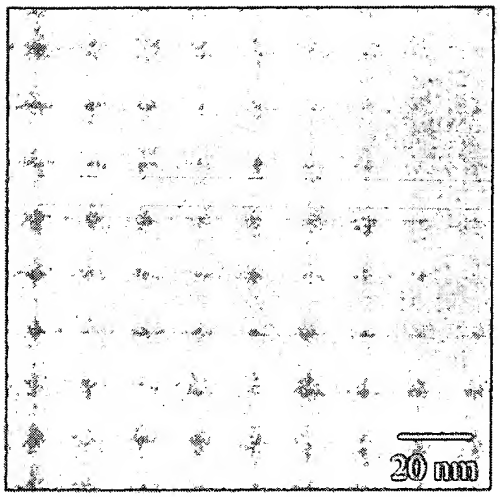

Figure 2. TEM image of a SWNT (diameter ~3 nm) grown from catalytic nanoparticles derived from ferritin.

the long loop segment is much lower, $\sim 8.6 \times 10^{-9}$ A/V, and the resistance is 2.7 MΩ at $V_g = -10$ V. These results combined with similar data acquired with other tubes suggest that the semiconducting nature of the nanotubes is retained along their lengths, indicating the absence of topological defects that cause apparent chirality change along the tube. Detailed length dependent transport properties and the effects of mechanical bending in the loop structures are being investigated currently.

To investigate the electronic nature of the SWNTs synthesized, we have measured 40 individual nanotubes with diameters ranging from 1 to 3 nm. It is known that SWNTs can be categorized into three types (Figure 4), truly metallic armchair SWNTs with (n,n) indices, semiconducting (m,n) SWNTs (S−SWNTs) with $m-n \neq 3\times integer$, and small band-gap semiconducting single-walled nanotubes (SGS−SWNTs) with $m-n = 3\times integer$ and $m \neq n$.[17−21] Considering all possible chiralities for SWNTs with diameters in the range of 1 to 3 nm, one identifies a total of 403 different nanotubes, as summarized in Table 1. If there is no preference in chirality, 3.5%, 31%, and 65.5% of the 403 nanotubes are metals, small gap tubes, and semiconductors, respectively.

Out of the 40 individual isolated SWNTs (Table 2), electrical transport measurements reveal that 25 (62.5%) are

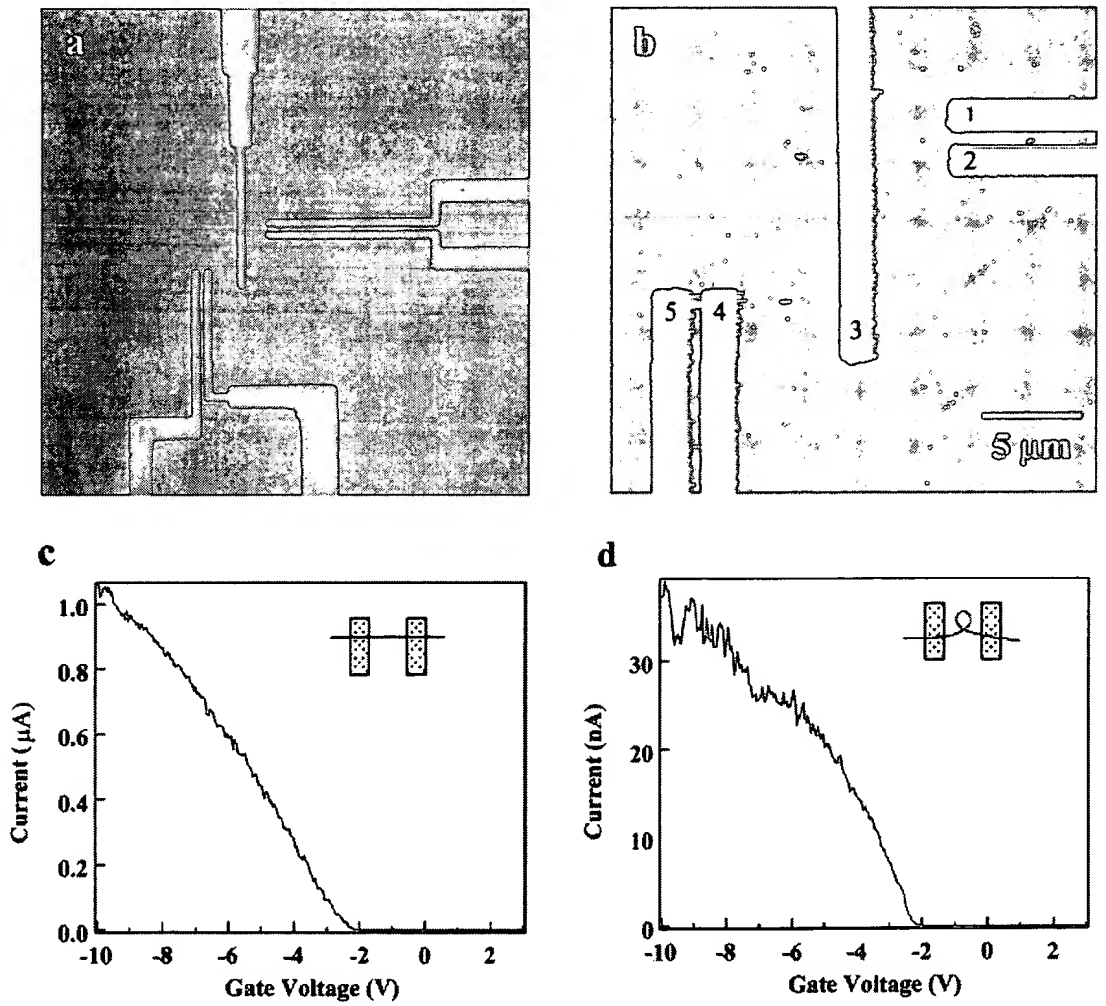

Figure 3. Multiprobe electrical measurements of long tubes. (a) Optical image of a device with five metal electrodes designed to contact a long SWNT. (b) AFM image showing the electrodes contacting the long nanotube with straight sections (between electrode pair: 1−2 and 5−4) and loop sections (between 2−3 and 3−4). (c) $I-V_g$ curve for a 700 nm long straight segment between 1 and 2 electrodes. (d) $I-V_g$ curve for a 21 μm long loop section between electrodes 2−3. Bias voltage = 100 mV.

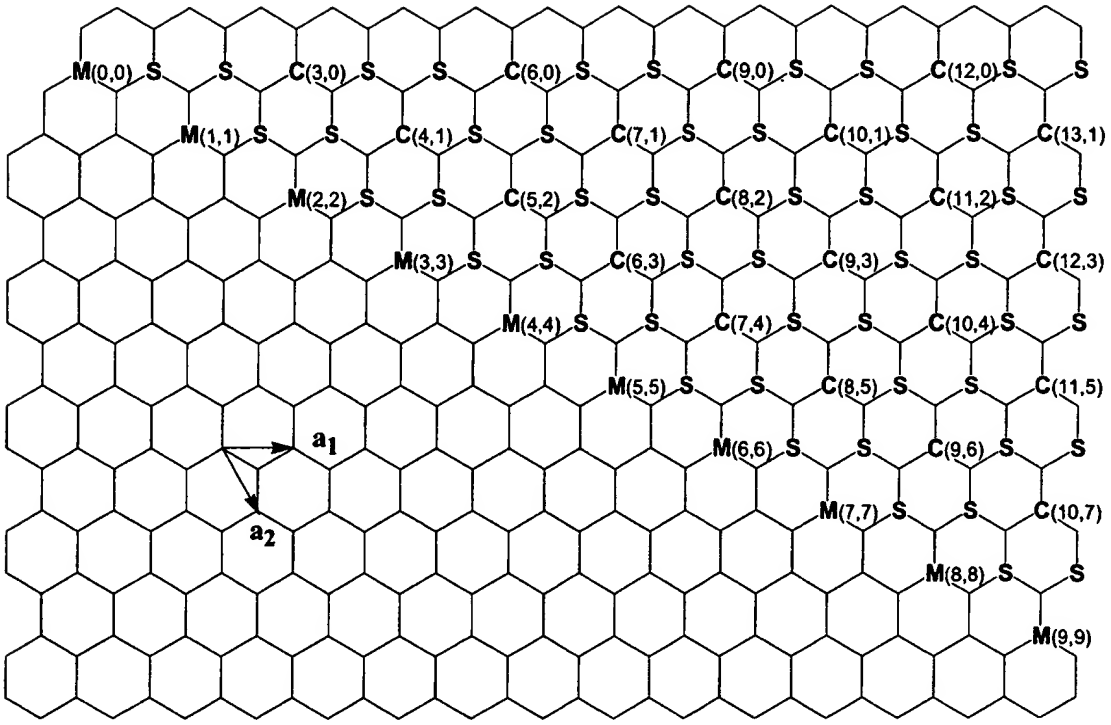

Figure 4. A map of chiral vectors that determine the chirality of SWNTs. Each vector is specified by the (*n*,*m*) indices. M, S, and C denote metals, semiconductors, and curvature induced small gap semiconducting SWNTs, respectively.

Table 1: Expected percentage of semiconductors, small band gap semiconductors, and metals for SWNTs with 1−3 nm diameters with no preference in chirality

	0−1 nm	1−2 nm	2−3 nm
S-SWNT	36 (62.1%)	100 (65.4%)	164 (65.6%)
SGS-SWNT	15 (25.9%)	46 (30.1%)	79 (31.6%)
M-SWNT	7 (12.1%)	7 (4.6%)	7 (2.8%)
total	58	153	250

Table 2: Experimentally revealed percentage of semiconductors, small band gap semiconductors, and metals for SWNTs (diameter = 1−3 nm) grown by CVD on ferritin-derived catalyst

	number of samples	percentage
S-SWNTs	25	62.5%
SGS-SWNTs	14	35.0%
M-SWNTs	1	2.5%
total	40	100.0%

semiconductors (S-SWNT) exhibiting characteristic conductance depletion by positive gate at room temperature (Figure 5a). Fourteen nanotubes (35%) exhibit a dip in the $I-V_g$ curve at room temperature, and the dip becomes a clear gap at low temperatures (Figure 5b). Such behavior has been observed previously and is attributed to small band gap (~10 meV) SWNTs.[22] Theoretically, the small band gaps arise for (*m*,*n*) tubes with $m-n = 3\times integer$ due to $\sigma-\pi$ orbital hybridization as a result of the nonflat nature of nanotube sidewalls.[18−21] The dip in $I-V_g$ at room temperature evolves into a depleted gap region at low temperature due to quenching of thermally excited charge carriers.[22] Only 1 out of the 40 SWNTs is assigned to an armchair metal tube showing weak gate dependence at room temperature and no conductance depletion region in the $I-V_g$ curve at low temperatures. Thus, the experimental survey reveals ~60−70% of S-SWNTs, 35% of SGS-SWNTs, and 2.5% of M-SWNTs (Table 2).

It is therefore concluded that our CVD growth conditions in fact produce SWNTs with no preference in chirality (Table 1). This result is not surprising considering the high growth temperature that can smear out the differences in thermodynamic energetics and kinetics for the growth of various chirality nanotubes. The initial nanotube nucleation process appears to be a determining step for tube chirality, after which the same chirality tends to be retained during nanotube lengthening in the base growth[1,2] mode. An important task then is to elucidate how various factors during nucleation determine the nanotube chirality by experiments and theory. These factors include growth temperature and structures of the nanoparticle seeds (diameter, shape, etc.). The interfacial structure between the nanoparticle and its supporting substrate could also play an important role. Understanding and controlling these factors will be indispensable to controlling nanotube chirality.

For device fabrication with CVD tubes, we have found large numbers of individual SWNTs that are FET-like semiconductors. The yield of metallic SWNT devices is quite low. Contrary to the CVD case, when experimenting with laser ablation[23] SWNTs, we observe a much higher percentage of nondepletable metallic SWNTs. Laser ablation does favor the growth of armchair tubes, a result that has been suggested by diffraction[23,24] measurements. Despite the lack of selectivity in chirality, the near 70% "natural abundance" of semiconductors in CVD SWNTs is welcome and places

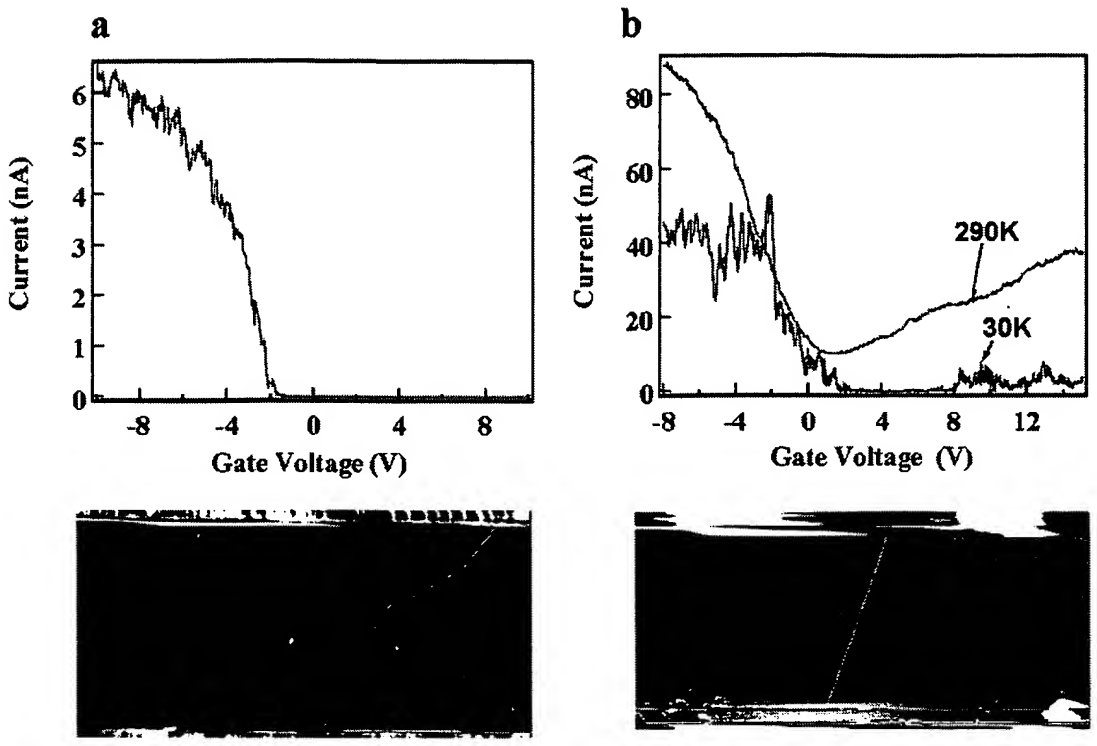

Figure 5. Representative $I-V_g$ curves recorded with (a) semiconducting SWNTs and (b) small band gap semiconducting SWNTs. Bias = 10 mV. The AFM images below the curves correspond to the single-nanotube devices. Top and bottom regions of the images are the edges of metal electrodes.

CVD nanotubes over laser materials for building transistors and sensors,[25-27] to which semiconductors are imperative. With patterned CVD growth, we are able to obtain small arrays of nanotube FETs in 100 × 100 μm^2 areas with ease. The yield for building such arrays with CVD approach is much higher than that obtainable with the approach of processing laser ablation SWNTs. Results of functional electronics and sensor arrays built with multiple-tube FETs will be presented in a future communication. We also note a useful application of the very long semiconducting SWNTs: they can be exploited for building large numbers of *identical* FETs and sensors along their lengths.

In summary, we have reported CVD synthesis of very long single-walled carbon nanotubes from well-defined catalyst nanoparticles patterned on SiO_2 substrates. The growth rate of SWNTs is found to be >60 μm/min. The long and slender SWNTs tend to form loops and closed rings along the lengths due to favorable van der Waals interactions between tube walls and high thermal energy at the growth temperature. These morphologies could be useful for exploring mesoscopic physics in quasi-1D ring structures. On the other hand, for certain applications, the ability of applying forces to nanotubes by electric fields during CVD[28] growth should allow the loop and ring formation to be manipulated or eliminated. Further, we have revealed that the CVD method produces high yield of semiconducting SWNTs. The natural abundance of semiconductors can already be exploited for building arrays of field effect transistors and sensors. We are currently exploring growth conditions that may shift the chirality distribution toward more semiconductors or metals. The task is daunting but worthwhile.

Acknowledgment. We thank useful discussions with Profs. C. Quate, J. Brauman, C. Chidsey, and N. Franklin. This work is supported by the MARCO MSD Focus Center, the Packard Foundation, the Sloan Foundation, a Terman Fellowship, and a Camile Dreyfus Teacher–Scholar Fellowship.

References

(1) Li, Y.; Kim, W.; Zhang, Y.; Rolandi, M.; Wang, D.; Dai, H. *J. Phys. Chem. B* **2001**, *105*, 11424–11431.
(2) Zhang, Y.; Li, Y.; Kim, W.; Wang, D.; Dai, H. *Appl. Phys. A* **2002**, *74*, 325–328.
(3) Cheung, C.; Kurtz, A.; Park, H.; Lieber, C. *J. Phys. Chem.* **2002**, *106*, 2429–2433.
(4) Dresselhaus, M. S.; Dresselhaus, G.; Eklund, P. C. *Science of Fullerenes and Carbon Nanotubes*; Academic Press: San Diego, 1996.
(5) Dai, H. *Surf. Sci.* **2002**, *500*, 218–241.
(6) Dai, H. In *Carbon Nanotubes*; Dresselhaus, M. S., Dresselhaus, G., Avouris, P., Eds.; Springer: Berlin, 2001; Vol. 80, pp 29–53.
(7) Choi, H.; Dai, H. *manuscript in preparation* **2002**.
(8) Kong, J.; Soh, H.; Cassell, A.; Quate, C. F.; Dai, H. *Nature* **1998**, *395*, 878.
(9) Soh, H.; Quate, C.; Morpurgo, A.; Marcus, C.; Kong, J.; Dai, H. *Appl. Phys. Lett.* **1999**, *75*, 627–629.
(10) Liu, J.; Dai, H. J.; Hafner, J. H.; Colbert, D. T.; Smalley, R. E.; Tans, S. J.; Dekker, C. *Nature* **1997**, *385*, 780–781.
(11) Martel, R.; HR, H. R. S.; P, P. A. *Nature* **1999**, *398*, 299.
(12) Sano, M.; Kamino, A.; Okamura, J.; Shinkai, S. *Science* **2001**, *293*, 1299–1301.
(13) Franklin, N. R.; Li, Y.; Chen, R. J.; Javey, A.; Dai, H. *Appl. Phys. Lett.* **2001**, *79*, 4571–4573.
(14) Franklin, N.; Dai, H. *Adv. Mater.* **2000**, *12*, 890.
(15) Tans, S.; Verschueren, A.; Dekker, C. *Nature* **1998**, *393*, 49–52.
(16) Chen, R.; Franklin, N.; Kong, J.; Cao, J.; Tombler, T.; Zhang, Y.; Dai, H. *Appl. Phys. Lett.* **2001**, *79*, 6951.
(17) Saito, R.; Fujita, M.; Dresselhaus, G.; Dresselhaus, M. S. *Appl. Phys. Lett.* **1992**, *60*, 2204.

(18) Hamada, N.; Sawada, S.-i.; Oshiyama, A. *Phys. Rev. Lett.* **1992**, *68*, 1579−1581.
(19) White, C. T.; Robertson, D. H.; Mintmire, J. W. In *Clusters and Nanostructured Materials*; Jena, P., Behera, S., Eds.; Nova: New York, 1996; p 231.
(20) Blase, X.; Benedict, L. X.; Shirley, E. L.; Louie, S. G. *Phys. Rev. Lett.* **1994**, *72*, 1878−1881.
(21) Kane, C. L.; Mele, E. J. *Phys. Rev. Lett.* **1997**, *78*, 1932−1935.
(22) Zhou, C.; Kong, J.; Dai, H. *Phys. Rev. Lett.* **2000**, *84*, 5604.
(23) Thess, A.; Lee, R.; Nikolaev, P.; Dai, H. J.; Petit, P.; Robert, J.; Xu, C. H.; Lee, Y. H.; Kim, S. G.; Rinzler, A. G.; Colbert, D. T.; Scuseria, G. E.; Tomanek, D.; Fischer, J. E.; Smalley, R. E. *Science* **1996**, *273*, 483−487.
(24) Cowley, J.; Nikolaev, P.; Thess, A.; Smalley, R. *Chem. Phys. Lett.* **1997**, *265*, 379−384.
(25) Kong, J.; Franklin, N.; Zhou, C.; Chapline, M.; Peng, S.; Cho, K.; Dai, H. *Science* **2000**, *287*, 622−625.
(26) Kong, J.; Chapline, M.; Dai, H. *Adv. Mater.* **2001**, *13*, 1384−1386.
(27) Kong, J.; Dai, H. *J. Phys. Chem.* **2001**, *105*, 2890−2893.
(28) Zhang, Y.; Chan, A.; Cao, J.; Wang, Q.; Kim, W.; Li, Y.; Morris, N.; Yenilmez, E.; Kong, J.; Dai, H. *Appl. Phys. Lett.* **2001**, *79*, 3155−3157.

NL025602Q